

**Two amino acid-templated metal phosphates: surfactant-thermal
synthesis, water stability, and proton conduction**

Lijuan Huang,^{a,b} Lei Wang,^{a,b} Yan Zhao,^a Ling Huang,^a Jian Bi,^a Guohong Zou,^b

Zhien Lin^{*b} and Daojiang Gao^{*a}

^a *College of Chemistry and Materials Science, Sichuan Normal University, Chengdu
610068, P. R. China.*

^b *College of Chemistry, Sichuan University, Chengdu 610064, P. R. China.*

* To whom correspondence should be addressed. Tel: +86-28-85412284. E-mail:

zhienlin@scu.edu.cn (Z. Lin); daojianggao@sicnu.edu.cn (D. Gao)

Physical measurements:

Powder X-ray diffraction (XRD) data were obtained using a Rigaku D/MAX-rA diffractometer with Cu-K α radiation ($\lambda = 1.5418 \text{ \AA}$). The elemental analysis was carried out on an Elementar Vario EL III analyzer. IR spectra (KBr pellets) were recorded on a Nicolet Impact 410 FTIR spectrometer. The thermogravimetric analyses were performed on a Netzsch STA 449c analyzer in a flow of N₂ with a heating rate of 10 °C/min. The fluorescent spectrum was collected on a Fluorolog-3 fluorescence spectrometer (Horiba JobinYvon) equipped with a 450 W xenon lamp. Alternating current impedance measurements were carried out with a Solartron SI 1260 impedance/gain-phase analyzer over the frequency range from 0.1 Hz to 10 MHz with an applied voltage of 10 mV. The relative humidity was controlled by a STIK Corp. CIHI-150B incubator. The sample was pressed to form a cylindrical pellet of crystalline powder sample (~2 mm thickness \times 5 mm ϕ) coated with C-pressed electrodes. Two silver electrodes were attached to both sides of pellet to form four end terminals (quasi-four-probe method). Single crystal X-ray diffraction data were collected on a New Gemini, Dual, Cu at zero, EosS2 diffractometer at room temperature. The crystal structures were solved by direct methods. The structures were refined on F^2 by full-matrix least-squares methods using the *SHELXTL* program package.¹

Reference

1. G. M. Sheldrick, *Acta Cryst., Sect. A*, 2008, 64, 112.

Synthesis

Synthesis of Zn(HPO₄)(C₆H₁₁NO₂) (1): Compound **1** was prepared by heating a mixture of ZnO (0.082 g), L-homoproline (0.261 g), H₃PO₄ (85%, 0.135 mL), and PEG-200 (2.0 mL) in a Teflon-coated steel autoclave at 150 °C for 7 days. The autoclave was subsequently allowed to cool to room temperature. Colourless crystals of compound **1** were separated from the resulting product by filtration, washed with ethanol, and dried in air (31% yield based on zinc). This compound can't be prepared

without L-homoproline in the reactions. Instead, a hydrated zinc phosphate $\text{Zn}_3(\text{PO}_4)_2 \cdot 4\text{H}_2\text{O}$ (hopeite, JCPDS: 37-465) was often obtained as the resulting product.

Synthesis of $(\text{C}_5\text{H}_{10}\text{NO}_2)\text{Ga}_4(\text{PO}_4)_4\text{F} \cdot 3\text{H}_2\text{O}$ (2): Compound **2** was prepared by heating a mixture of Ga_2O_3 (0.187 g), L-proline (0.115 g), H_3PO_4 (85%, 0.135 mL), HF (40%, 88 μL), and PEG-200 (2.0 mL) in a Teflon-coated steel autoclave at 160 °C for 7 days. The autoclave was subsequently allowed to cool to room temperature. Light-yellow crystals of compound **2** were separated from the resulting product by filtration, washed with ethanol, and dried in air (46% yield based on gallium). This compound can't be prepared without L-proline in the reactions. Instead, a dense gallium phosphate GaPO_4 with a quartz-type structure was often obtained as the resulting product.

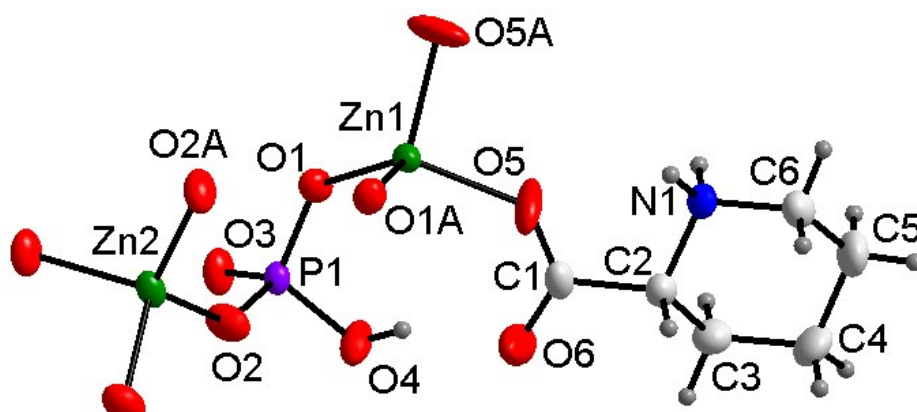


Fig. S1. View of the tetrahedral coordination environments for Zn and P in the asymmetric unit of compound **1**, showing the atom-labeling scheme and 50% thermal ellipsoids. Atom labels having “A” and “B” refer to symmetry-generated atoms.

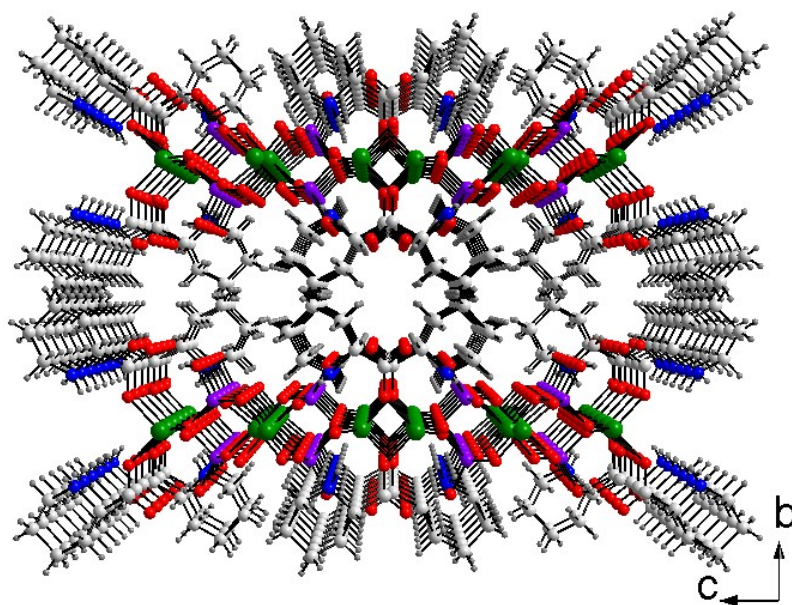


Fig. S2. Pack structure of compound **1** along the $[100]$ direction.

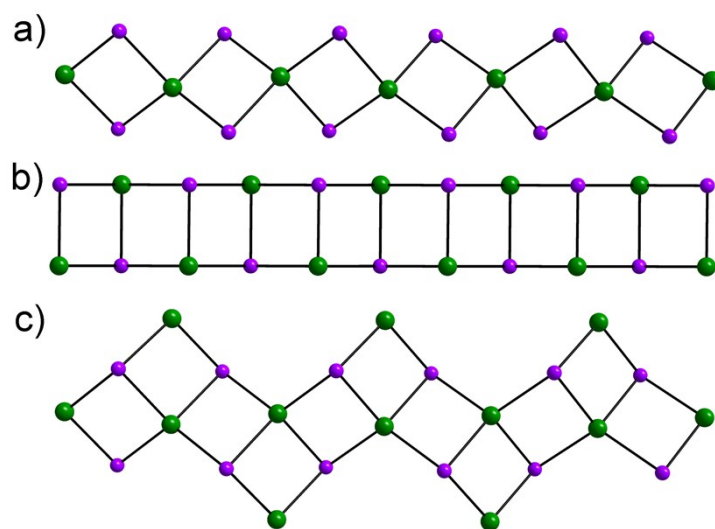


Fig. S3. Schematic representation of three chain-like structures found in metal phosphates: (a) corner-sharing 4-MR chain; (b) edge-sharing 4-MR chain; (c) zigzag edge-sharing 4-MR chain. Oxygen atoms are omitted for clarity.

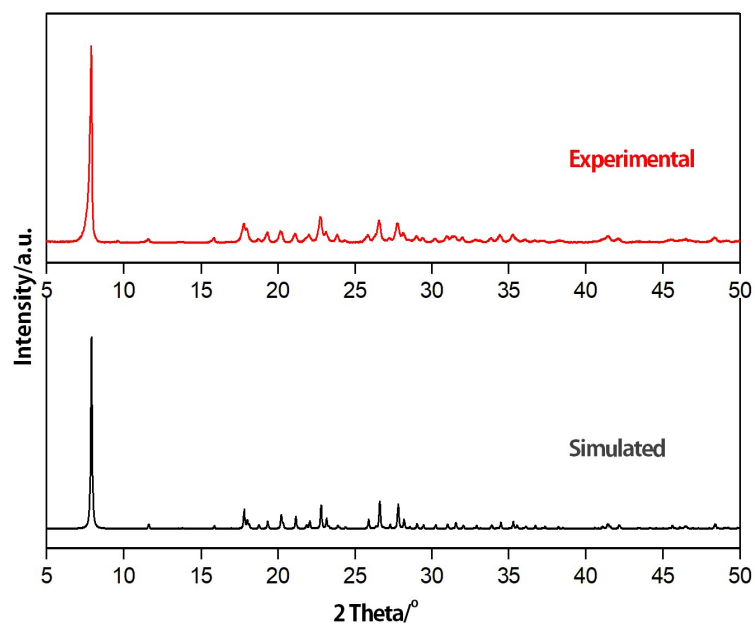


Fig. S4. Experimental and simulated powder XRD patterns of compound **1**.

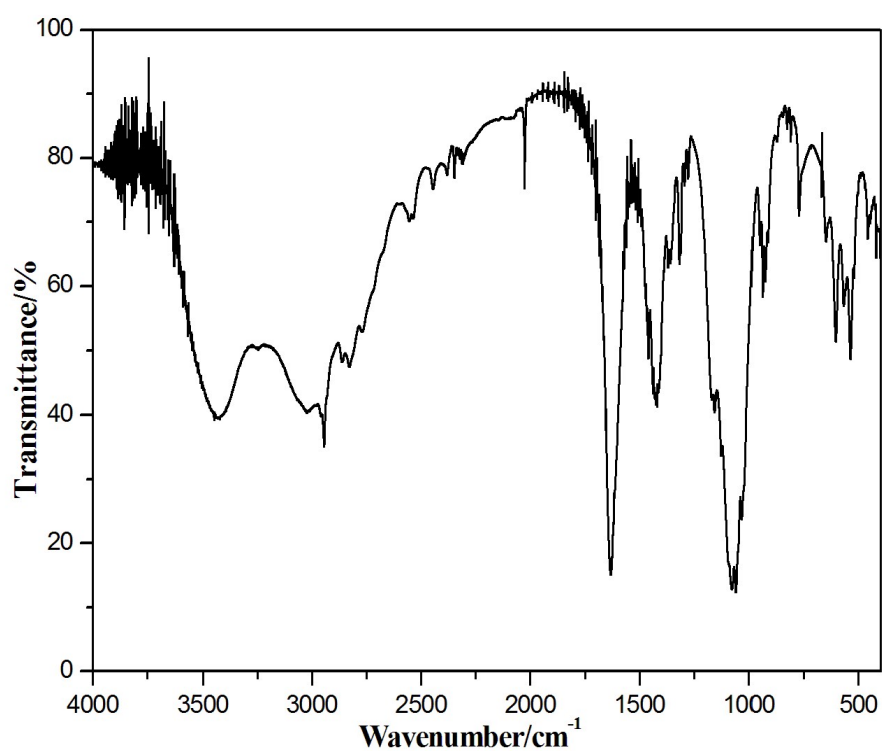


Fig. S5. IR spectrum of compound **1**.

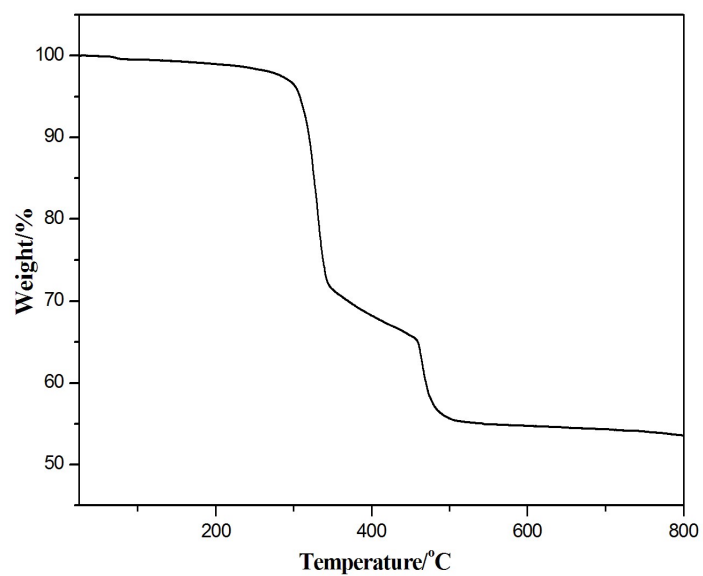


Fig. S6. TGA curve of compound 1.



Fig. S7. Crystal photo of compound 1 on a thin glass fiber.

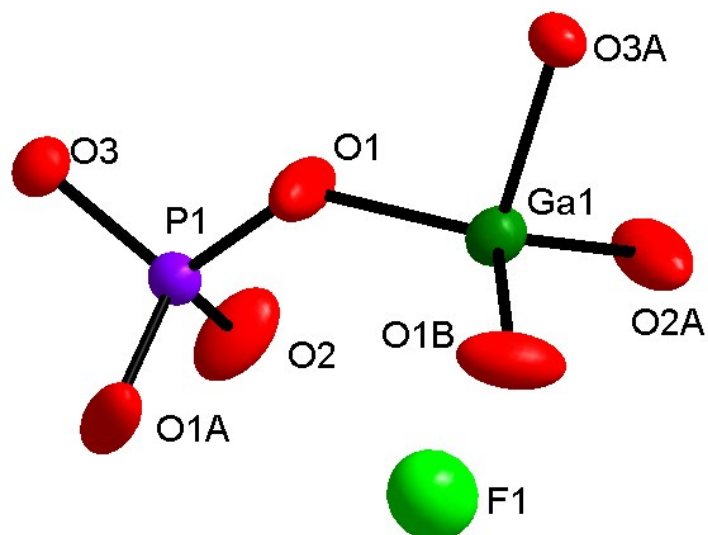


Fig. S8. View of the tetrahedral coordination environments for Ga and P in the asymmetric unit of compound **2**, showing the atom-labeling scheme and 50% thermal ellipsoids. Atom labels having “A” and “B” refer to symmetry-generated atoms.

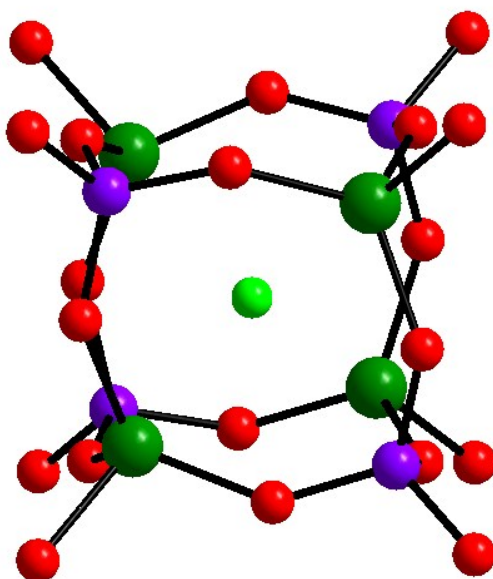


Fig. S9. View of the d4r cage encapsulating F⁻ ions within its center.

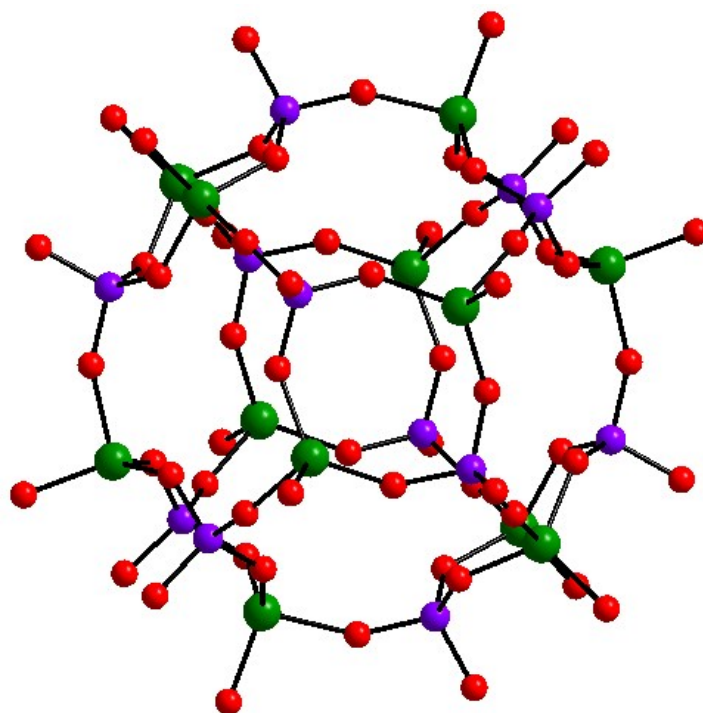


Fig. S10. View of the β cage in compound 2.

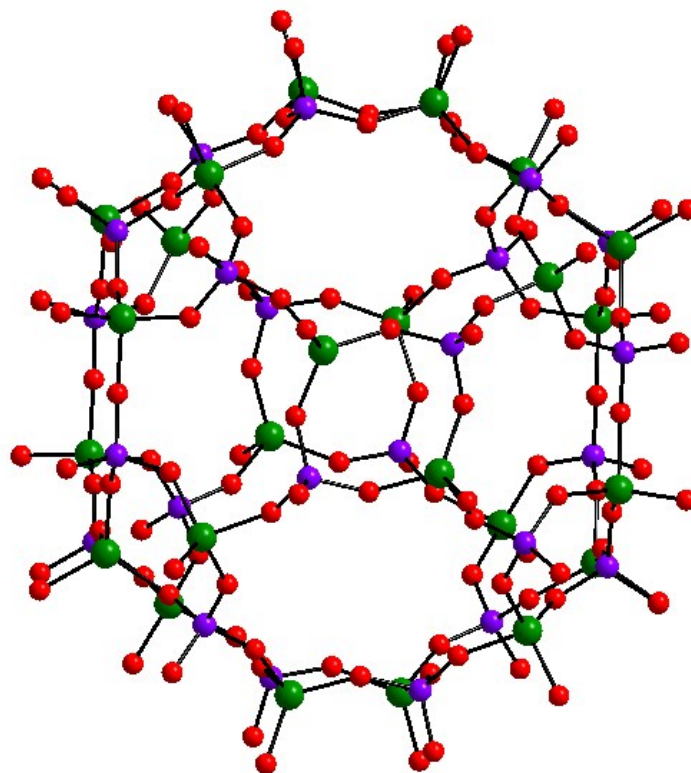


Fig. S11. View of the α cage in compound 2.

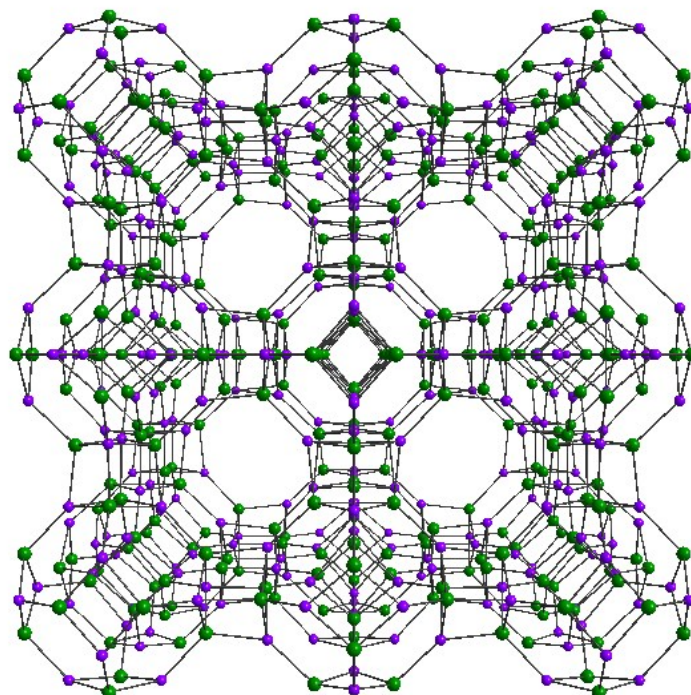


Fig. S12. The zeolitic LTA topology of compound 2.

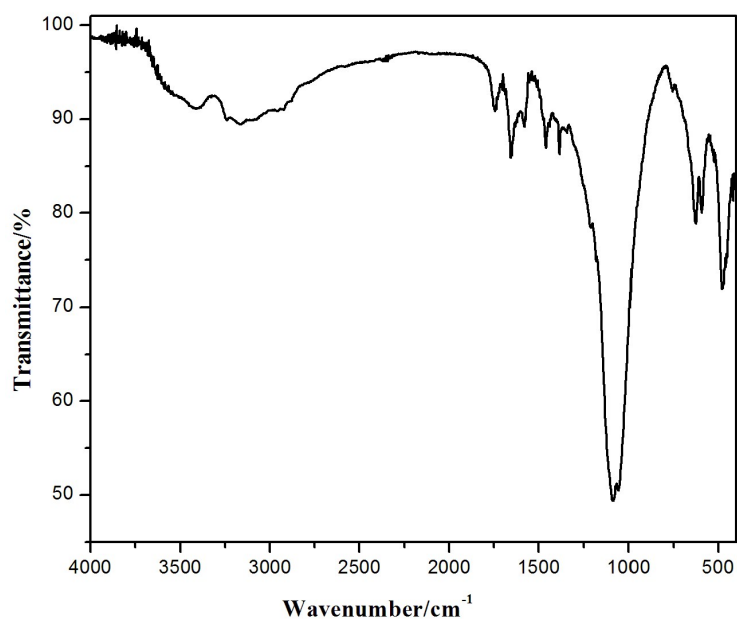


Fig. S13. IR spectrum of compound 2.

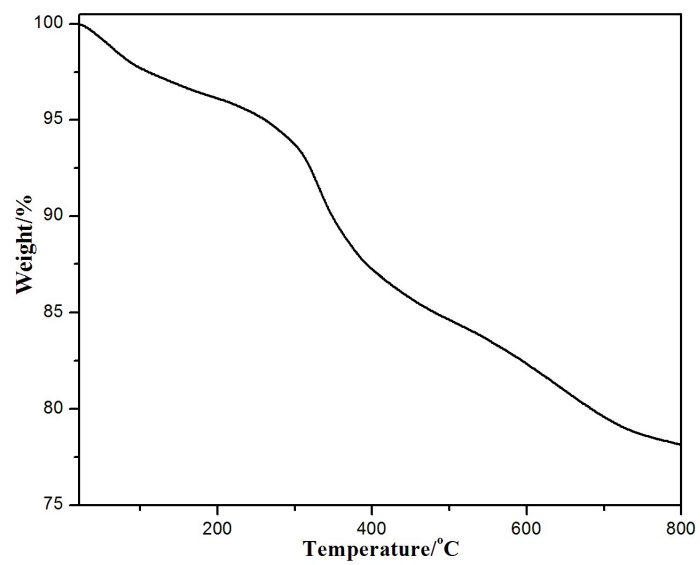


Fig. S14. TGA curve of compound 2.

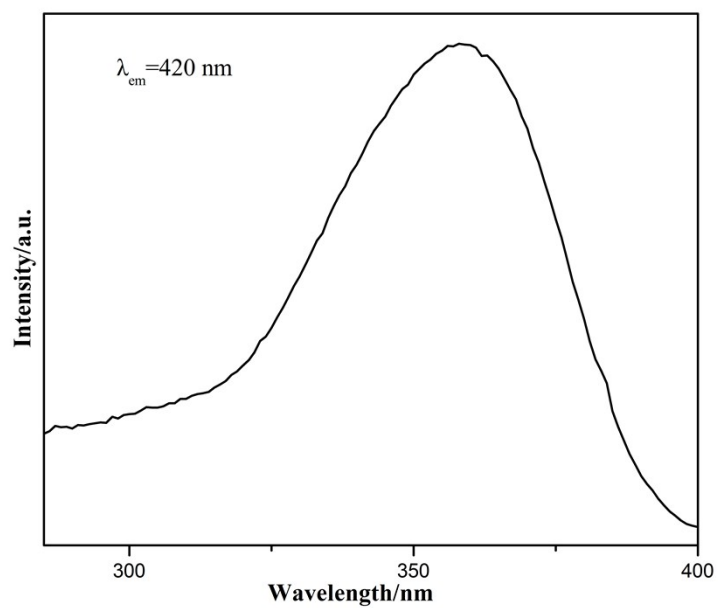


Fig. S15. The excitation spectrum of compound 2.

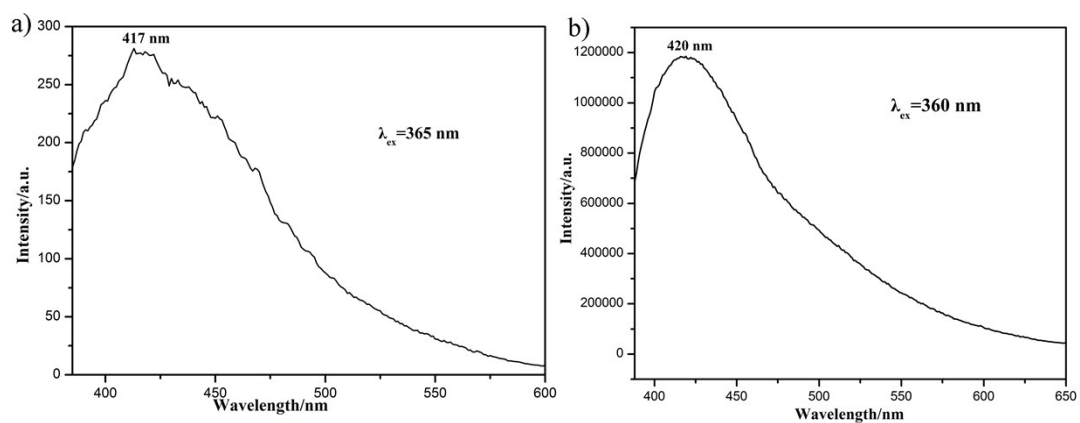


Fig. S16. Room-temperature emission spectra of (a) L-proline molecules and (b) compound 2.

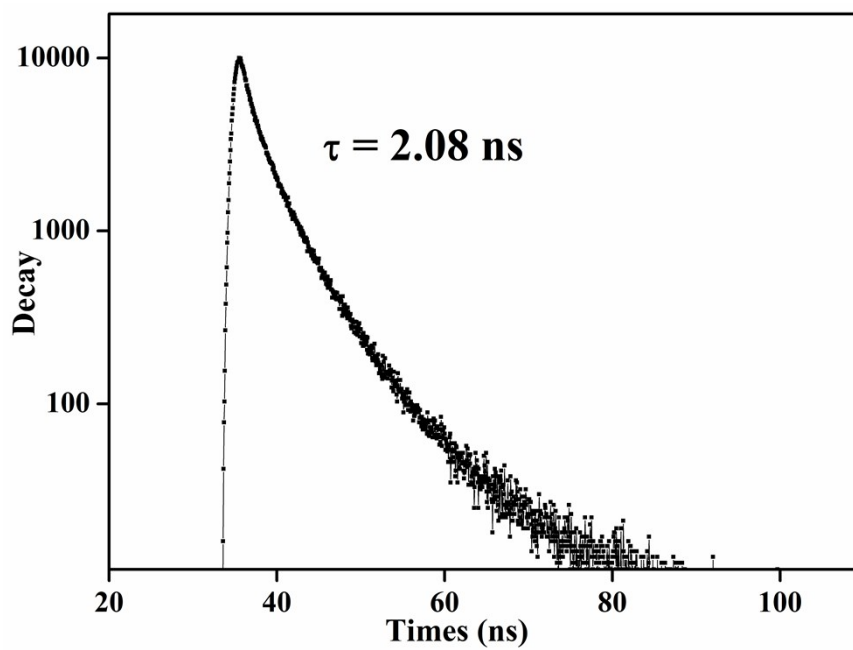


Fig. S17. The lifetime of compound 2.

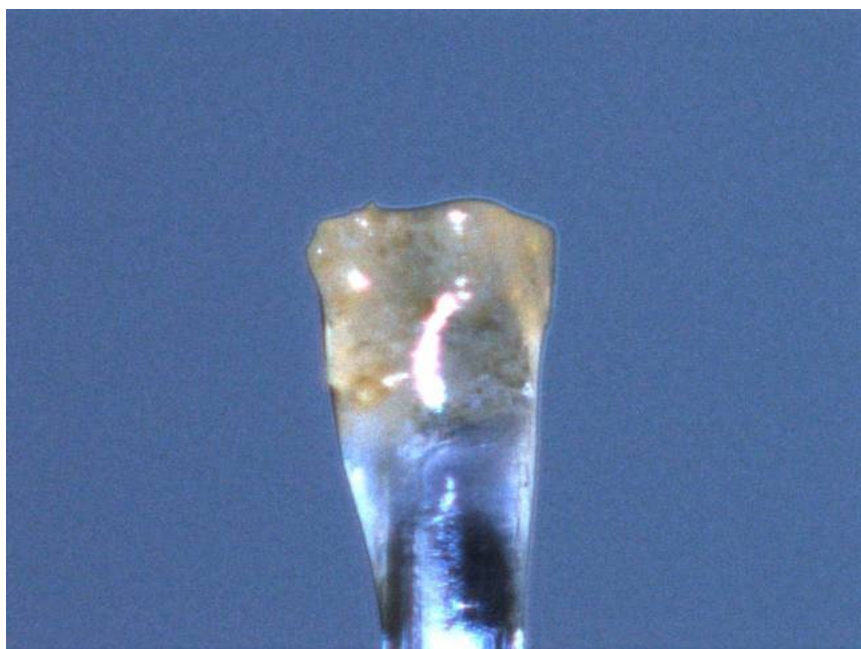


Fig. S18. Crystal photo of compound **2** on a thin glass fiber.

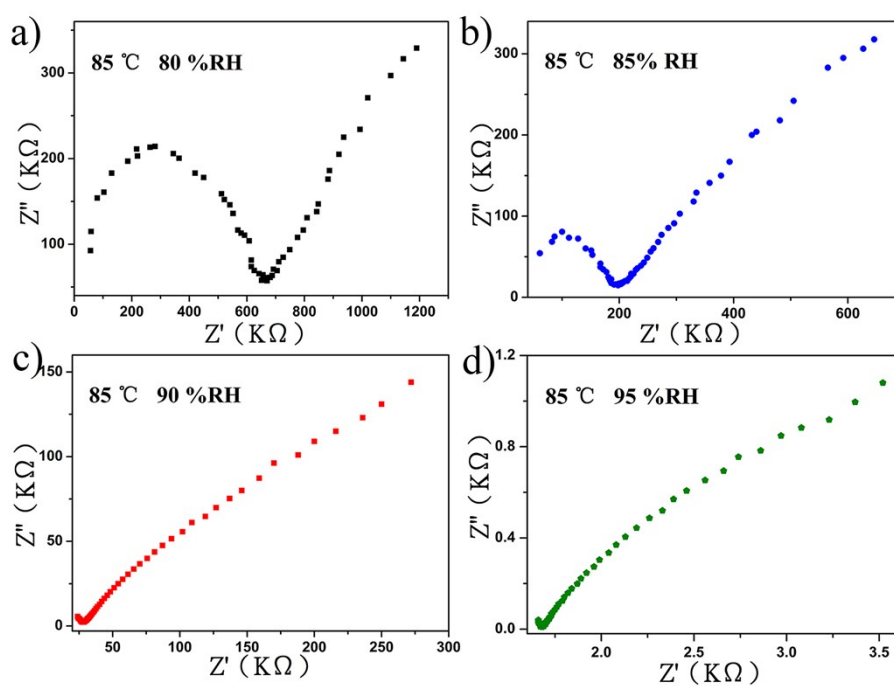


Fig. S19. Nyquist plots of compound **2** at 85 °C under different humidity conditions. The conductivity is $2.29 \times 10^{-6} \text{ S}\cdot\text{cm}^{-1}$ (80% RH), $7.54 \times 10^{-6} \text{ S}\cdot\text{cm}^{-1}$ (85% RH), $4.43 \times 10^{-5} \text{ S}\cdot\text{cm}^{-1}$ (90% RH), and $8.89 \times 10^{-4} \text{ S}\cdot\text{cm}^{-1}$ (95% RH).